

# Hybrid III–V on Silicon Lasers for Photonic Integrated Circuits on Silicon

Guang-Hua Duan, *Senior Member, IEEE*, Christophe Jany, Alban Le Liepvre, Alain Accard, Marco Lamponi, Dalila Make, Peter Kaspar, Guillaume Levaufre, Nils Girard, François Lelarge, Jean-Marc Fedeli, Antoine Descos, Badhise Ben Bakir, Sonia Messaoudene, Damien Bordel, Sylvie Menezo, Guilhem de Valicourt, Shahram Keyvaninia, Gunther Roelkens, Dries Van Thourhout, David J. Thomson, Frederic Y. Gardes, and Graham T. Reed

(Invited Paper)

**Abstract**—This paper summarizes recent advances of integrated hybrid InP/SOI lasers and transmitters based on wafer bonding. At first the integration process of III–V materials on silicon is described. Then the paper reports on the results of single wavelength distributed Bragg reflector lasers with Bragg gratings etched on silicon waveguides. We then demonstrate that, thanks to the high-quality silicon bend waveguides, hybrid III–V/Si lasers with two integrated intra-cavity ring resonators can achieve a wide thermal tuning range, exceeding the C band, with a side mode suppression ratio higher than 40 dB. Moreover, a compact array waveguide grating on silicon is integrated with a hybrid III–V/Si gain section, creating a wavelength-selectable laser source with 5 wavelength channels spaced by 400 GHz. We further demonstrate an integrated transmitter with combined silicon modulators and tunable hybrid III–V/Si lasers. The integrated transmitter exhibits 9 nm wavelength tunability by heating an intra-cavity ring resonator, high extinction ratio from 6 to 10 dB, and excellent bit-error-rate performance at 10 Gb/s.

**Index Terms**—Hybrid photonic integrated circuits, silicon laser, semiconductor lasers, silicon-on-insulator (SOI) technology, adiabatic taper.

Manuscript received October 6, 2013; revised December 20, 2013; accepted December 22, 2013. Date of publication January 2, 2014; date of current version February 6, 2014. This work was supported in part by the European FP7 Helios project, and the French national ANR projects Micros, Silver and Ultimate.

G.-H. Duan, C. Jany, A. L. Liepvre, A. Accard, M. Lamponi, D. Make, P. Kaspar, G. Levaufre, N. Girard, and F. Lelarge are with the III-V Lab, 91767 Palaiseau cedex, Paris, France (e-mail: guanghua.duan@3-5lab.fr; christophe.jany@3-5lab.fr; alban.liepvre@3-5lab.fr; alain.accard@3-5lab.fr; marco.lamponi@3-5lab.fr; Dalila.Make@3-5lab.fr; peter.kaspar@3-5lab.fr; guillaume.levaufre@3-5lab.fr; nils.girard@3-5lab.fr; francois.lelarge@3-5lab.fr).

J.-M. Fedeli, A. Descos, B. Ben Bakir, S. Messaoudene, D. Bordel, and S. Menezo are with the CEA/Leti, LETI, MINATEC, 38054 Grenoble cedex 9, France (e-mail: jean-marc.fedeli@cea.fr; antoine.descos@cea.fr; badhise.ben-bakir@cea.fr; sonia.messaoudene@cea.fr; damien.bordel@cea.fr; sylvie.menezo@cea.fr).

G. de Valicourt is with the Bell Laboratories, WDM Dynamic Networks Department, 91620 Nozay, France (e-mail: Guilhem.De\_Valicourt@alcatel-lucent.com).

S. Keyvaninia, G. Roelkens, and D. Van Thourhout are with the Photonic Research Group, INTEC, Ghent University-IMEC, 9000 Ghent, Belgium (e-mail: Shahram.Keyvaninia@intec.ugent.be; gunther.roelkens@intec.ugent.be; dries.vanthourhout@intec.ugent.be).

D. J. Thomson, F. Y. Gardes, and G. T. Reed are with the Optoelectronics Research Centre, University of Southampton, Southampton, SO17 1BJ, U.K. (e-mail: d.thomson@soton.ac.uk; f.gardes@soton.ac.uk; g.reed@soton.ac.uk).

Color versions of one or more of the figures in this paper are available online at <http://ieeexplore.ieee.org>.

Digital Object Identifier 10.1109/JSTQE.2013.2296752

## I. INTRODUCTION

SILICON photonics is attracting a lot of attention due to the prospect of low-cost, compact circuits that integrate photonic and microelectronic elements on a single chip [1], [2]. It can address a wide range of applications from short-distance data communication to long-haul optical transmission [3]. Today, practical Si-based light sources are still missing, despite the recent promising demonstration of an optically pumped germanium laser [4], [5]. This situation has propelled research on heterogeneous integration of III–V semiconductors with silicon through wafer bonding techniques [6]–[8]. In this approach, unstructured InP dies or wafers are bonded, epitaxial layers facing down, on a silicon-on-insulator (SOI) waveguide circuit wafer, after which the InP growth substrate is removed and the III–V epitaxial film is processed. Such an approach exploits the highly efficient light emission properties of some direct-gap III–V semiconductor materials such as compounds based on GaAs and InP.

Important achievements have been made in the past on the heterogeneous integration of III–V on silicon as reported in [6]–[8]. Two different waveguide structures for the hybrid III–V/Si integration have been investigated. In the first one, as described in [6] and [8], the mode is mainly guided by the Si waveguide and evanescently couples with the III–V waveguide, using a very thin bonding layer (<5 nm, corresponding to the Si native oxide). In the second one described in [7], the mode in the hybrid section is mainly guided by the III–V waveguide, and the light is coupled from the III–V waveguide to the silicon waveguide through waveguide tapering. In this case, the bonding interface can be relatively thick (from 30 to 150 nm, typically). The advantage is that the optical mode experiences a high optical gain in the central region of the laser structure. This paper will focus on the second waveguide structure, and will demonstrate that efficient mode transfer can be achieved between III–V and silicon waveguide [9], [10]

Large progress has also been made in the past on the emission spectrum control. For instance, distributed feedback (DFB) and distributed Bragg reflector (DBR) lasers with single longitudinal mode emission have been reported in [8]. In those lasers, the Bragg gratings are etched on silicon waveguides by keeping the III–V waveguide as simple as possible. More recently, wavelength tunable lasers with large tuning range have

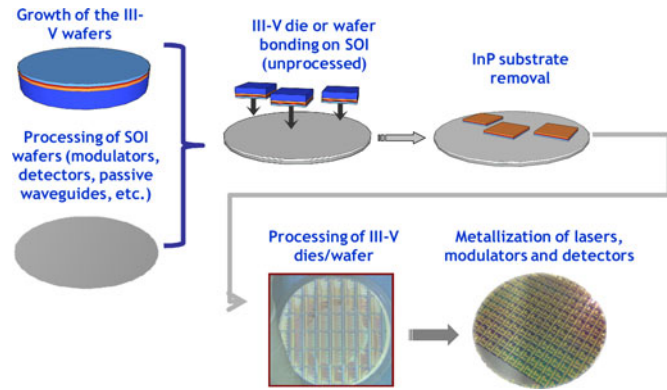


Fig. 1. Process flow of heterogeneous integration of III-V on silicon.

been published, showing very promising results [11]–[13]. We demonstrate that the use of two silicon ring resonators (RRs) allows us to achieve a tuning range of more than 45 nm and a side mode suppression ratio (SMSR) larger than 40 dB over the entire tuning range [11].

Thanks to the mature silicon fabrication process, even more complicated silicon waveguides structures can be integrated within a hybrid III-V/Si laser and used for laser wavelength control. For instance, an arrayed waveguide grating (AWG) filter can be integrated in a laser cavity, together with several semiconductor optical amplifiers (SOA), in order to make an AWG laser. The first AWG laser on Si was reported in [14] with 4 channels spaced by 360 GHz. The threshold current ranged from 113 to 147 mA, and the output power to a fibre from  $-23$  to  $-14.5$  dBm. We recently demonstrated a 5-channel AWG laser with 392 GHz separation [15], and also a 4-channel AWG laser with 200 GHz channel spacing [16]. The threshold current ranged from 38 to 42 mA, and the output power in a single-mode fibre from  $-8.4$  to  $-2.2$  dBm.

Integrated transmitters incorporating lasers and modulators on silicon are of primary importance for all communication applications, and at the same time are the most challenging to fabricate due to the need of hybrid III-V integration. The first demonstration of such a photonic integrated circuit (PIC) was reported by A. Alduino *et al.* [17]. This silicon PIC transmitter is composed of hybrid III-V/silicon lasers and silicon Mach-Zehnder modulators (MZM) operating in the wavelength window of  $1.3 \mu\text{m}$ . However, wavelength-division-multiplexing applications usually require wavelength-tunable laser sources. Moreover, tunable transmitters are considered to be an attractive option in optical network terminal transceivers for future access networks. The very large market of access networks provides an opportunity for silicon photonics. We reported for the first time on an integrated tunable laser MZM (ITLMZ) operating in the wavelength window of  $1.5 \mu\text{m}$ , which combines a tunable hybrid III-V/Si laser and a silicon MZ modulator [18]. Our ITLMZ demonstrates several new features: i) wavelength tunability over 9 nm; ii) a silicon modulator with high extinction ratio (ER) between 6 and 10 dB, and 3 dB modulation bandwidth as large as 13 GHz; and iii) excellent bit-error rate (BER) performance.

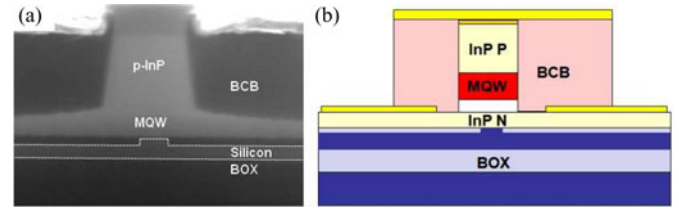


Fig. 2. (a) Cross-sectional SEM picture of a hybrid waveguide with white lines added to make the silicon waveguide visible. (b) Schematic cross section.

This paper will summarize our recent advances on integrated hybrid InP/SOI lasers and transmitters based on wafer bonding. It is organized as follows. Section II is devoted to the heterogeneous integration process of III-V material on silicon, including one of the key points of hybrid III-V/Si lasers: the optical mode transition from III-V to silicon waveguides. Section III gives the results of single-wavelength DBR lasers with high output power. Section IV will focus on wavelength-tunable lasers, and Section V on wavelength-selectable AWG lasers. Section VI reports on the performance of an ITLMZ operating at 10 Gb/s. Finally, a conclusion is drawn in Section VII.

## II. HETEROGENEOUS INTEGRATION OF III-V ON SILICON

### A. Heterogeneous Integration Process of III-V Material on Silicon

Fig. 1 outlines the process flow for silicon PICs using the heterogeneous integration of III-V material on Si.

The fabrication starts with 200 mm SOI wafers with a typical thickness of 440 nm thick silicon top layer. The first step is the formation of passive rib waveguides by etching the top silicon layer. These waveguides are optimized for the coupling with III-V waveguides that will be aligned on top of the silicon waveguides in a later step. After this etching step, the remaining silicon layer has a thickness of 220 nm. For the passive circuitry, additional etching steps are applied to form strip waveguides and other elements such as Bragg reflectors or vertical output couplers. To planarize the surface of the SOI wafer, a silica layer is deposited and a chemical-mechanical polishing is applied [19].

In the meantime, 2" InP wafers are grown. The III-V region consists of a p-InGaAs contact layer, a p-InP cladding layer, typically 6 InGaAsP quantum wells surrounded by two InGaAsP separate confinement heterostructure layers, and an n-InP layer. Optimized growth conditions have been established in order to simultaneously achieve a defect-free surface morphology required for bonding and high laser performances. These InP wafers can now be bonded onto the SOI wafers [20].

After wafer bonding and InP substrate removal, dry etching is used to etch through the InGaAs layer and partly etch the InP p-doped waveguide cladding layer. The InP etching is completed by chemical selective etching. The MQW layer is etched by  $\text{CH}_4:\text{H}_2$  RIE. Fig. 2 shows a scanning electron microscope (SEM) picture of a III-V waveguide on top of a silicon waveguide.

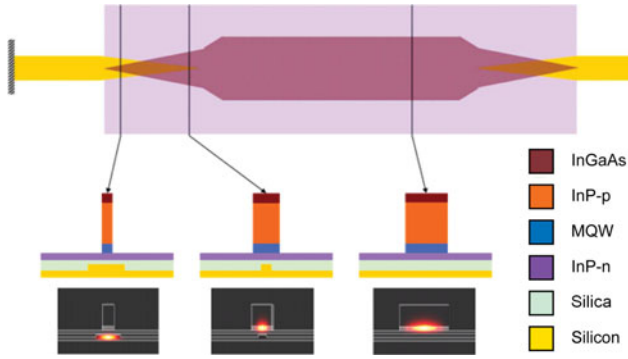


Fig. 3. Top and cross-sectional views of the coupling structure of the hybrid laser with representative mode profiles in three cross-sections.

The active waveguide is encapsulated with DVS-benzocyclobutene. A Ti/Pt/Au alloy is used for metallization on both p and n sides. Finally, the fabricated lasers are ready to be tested on the wafer through the use of vertical grating couplers.

### B. Adiabatic Coupling Between III-V and Silicon Waveguides

Fig. 3 gives a schematic view of the laser structure, which can be divided into three parts. In the center of the device the optical mode is confined to the III-V waveguide, which provides the optical gain. At both sides of this section there is a coupling region that couples light from the III-V waveguide to the underlying silicon waveguide. After the coupling region the light is guided by a silicon waveguide without III-V on top.

The intensity profiles of the fundamental mode are calculated using the film mode matching method, and are given in Fig. 3 at different points of the laser cavity. The calculated optical confinement in the MQW layer in the center of the laser cavity is in the range between 5% and 12%.

To achieve index matching between the two waveguides, a deep ridge III-V waveguide is usually used in the double taper region. As shown in Fig. 3, a double taper structure is used to allow the efficient coupling of the fundamental mode from the III-V waveguide to the silicon waveguide [10]. In the right double taper region, the silicon waveguide has an increasing width, while the III-V waveguide's width is decreasing. Fig. 4 shows the coupling efficiency of the double adiabatic taper for three values of the III-V tip width: 0.4, 0.8 and 1  $\mu\text{m}$  and a silicon waveguide thickness of 400 nm. We can see that perfect coupling can only be achieved using a tip width of 0.4  $\mu\text{m}$  or less. This requirement on the tip width is linked to the 400 nm silicon waveguide thickness. For thicker silicon waveguides a larger tip width can be tolerated. We can also observe highly efficient coupling for short taper length (around 30  $\mu\text{m}$ ). However, the coupling efficiency varies quickly with the taper length and other parameters for such a short taper. Longer ( $> 100 \mu\text{m}$ ) tapers are preferred in order to get more robust coupling.

In the case of thicker silicon waveguides ( $\geq 500 \text{ nm}$ ), only the silicon waveguide needs to be tapered for the mode-transfer from the III-V waveguide to the silicon waveguide [9]. As narrow

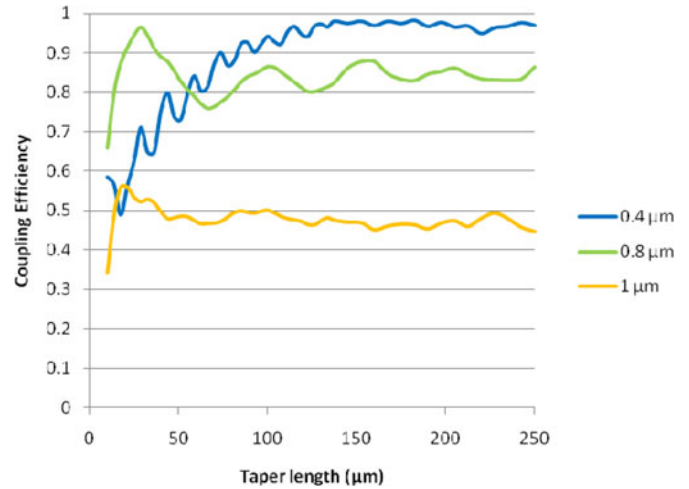


Fig. 4. Coupling efficiency for different III-V taper tip widths as a function of the double taper length.

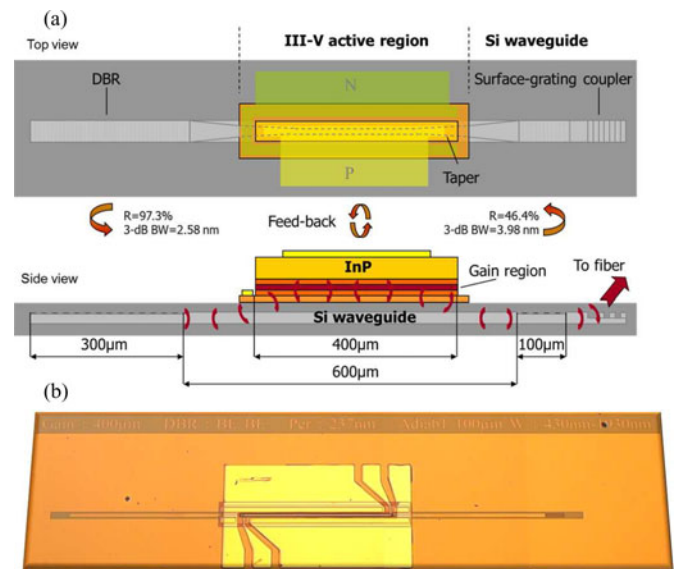


Fig. 5. a) Schematic representations of the hybrid III-V/Si laser, top and side views. b) Optical microscope image of the final fabricated device.

III-V tapers are no longer required, the process of III-V waveguides becomes much more tolerant.

## III. SINGLE MODE DBR LASERS

### A. DBR Laser Structure

In this section, we report on the experimental demonstration of a heterogeneously integrated III-V/Si DBR laser with low threshold ( $< 20 \text{ mA}$ ) and high output power ( $> 15 \text{ mW}$ ). The laser performances are similar to those obtained by A. J. Zilkie *et al.* who built a hybrid external-cavity DBR laser from a III-V reflective SOA butt-coupled to a 3  $\mu\text{m}$ -thick Si waveguide containing a Bragg grating reflector [21].

The optical cavity is defined by a III-V gain section of 400  $\mu\text{m}$  length and two DBRs spaced 600  $\mu\text{m}$  apart, as shown in Fig. 5. The Bragg grating was etched into a silicon waveguide with a width of 10  $\mu\text{m}$ . The grating pitch is 237 nm and the duty cycle

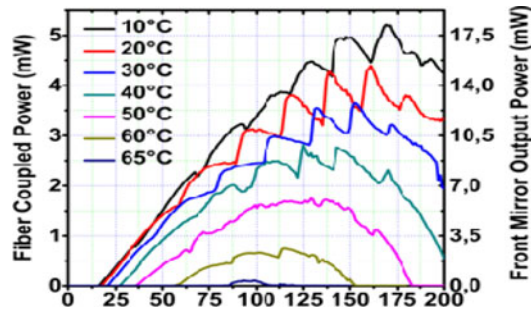


Fig. 6.  $L$ - $I$  characteristics of the hybrid DBR laser for different temperatures.

is 50%. The etching depth is chosen to be only 10 nm, resulting in a reasonable grating coupling coefficient,  $\kappa$ , of  $83 \text{ cm}^{-1}$ . The back-side Bragg grating has a length of  $300 \mu\text{m}$ , leading to a calculated modal reflectivity of 97.3% and a 3 dB bandwidth of 2.58 nm. The front-side Bragg grating has a length of  $100 \mu\text{m}$ . From calculation, this Bragg grating has a modal reflectivity of 46.4% and a 3 dB bandwidth of 3.98 nm. The combined Bragg gratings lead to a sufficiently narrow filter to allow single longitudinal mode operation of the DBR laser.

### B. Experimental Results

The continuous wave laser output power is collected through a surface-grating coupler by a multimode fiber and then characterized by using both a spectrum analyzer and an optical power meter. To determine the output power at the low-reflectivity side of the hybrid DBR laser, we measured the insertion losses using a reference structure on the same wafer.

Fig. 6 shows the fiber-coupled and front mirror output power-current ( $L$ - $I$ ) characteristics for operating temperatures ranging from 15 to  $65^\circ\text{C}$ . As can be seen from the  $L$ - $I$  curves, the laser threshold is 17 mA with a maximum output power of 15 mW at  $20^\circ\text{C}$  ( $> 4 \text{ mW}$  in the fiber), leading to a differential quantum efficiency of 13.3%. The differential quantum efficiency is defined as the derivative of the  $L$ - $I$  curve, multiplied by  $e/h\nu$ , with  $e$  the electron charge and  $h\nu$  the photon energy. It operates up to a stage temperature of  $60^\circ\text{C}$  with a front mirror output power exceeding 2.4 mW.

The lasing spectrum for a drive current of 118 mA is shown in Fig. 7. We can see that there is a dominant mode at 1546.97 nm, with a SMSR of about 50 dB.

Fig. 8 shows the lasing spectrum as a function of the drive current along with the corresponding  $L$ - $I$ - $V$  curves. Measurements were performed at room temperature. We can see that the device has a lasing turn-on voltage of 1.0 V and a series resistance of  $7.5 \Omega$ . From the optical spectrum, we can clearly observe jumps in the lasing longitudinal mode due to mode hops. This is due to the fact that the increase of the injection current into the gain section results in an increase of the temperature of the III-V waveguide. Consequently the refractive index of the III-V materials increases, leading to a red shift of the longitudinal mode of the hybrid DBR laser. When the lasing mode is far enough from the reflectivity peak, the dominant longitudinal

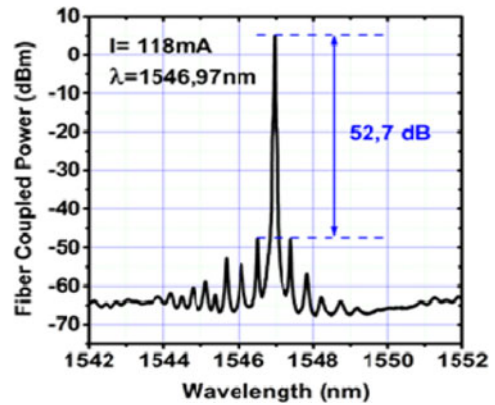


Fig. 7. Lasing spectrum measured at a bias current of 118 mA.

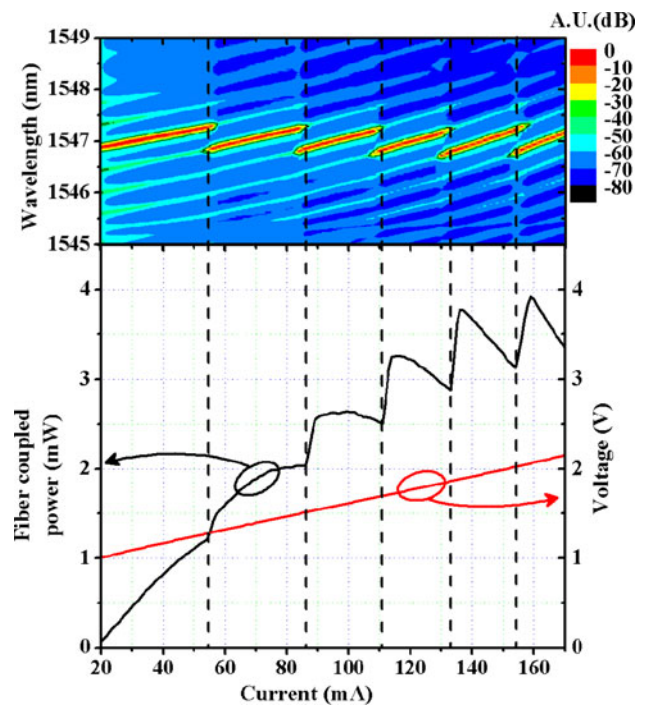


Fig. 8. Fiber-coupled  $L$ - $I$ - $V$  characteristic and normalized contour plot of the lasing spectra at room temperature.

mode hops to another mode closer to the reflection peak of the Bragg grating.

The small-signal modulation response of the laser is shown in Fig. 9. One can observe a flat response at low frequencies and also resonance due to relaxation oscillations. The 3 dB bandwidth of around 7 GHz is obtained for bias currents ranging from 125 mA to 150 mA.

## IV. WAVELENGTH TUNABLE LASERS

### A. Design and Fabrication

The tunable laser, as schematically shown on Fig. 10 (top), consists of an InP-based amplification section, tapers for the modal transfer between III-V and Si waveguides, two RRs for single mode selection, metal heaters on top of the rings for the thermal wavelength tuning and Bragg gratings providing

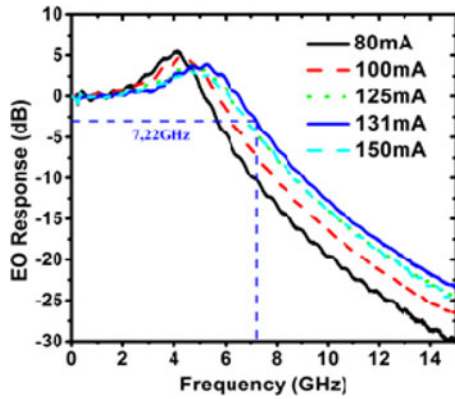


Fig. 9. Room temperature frequency response of the hybrid DBR laser for different bias currents.

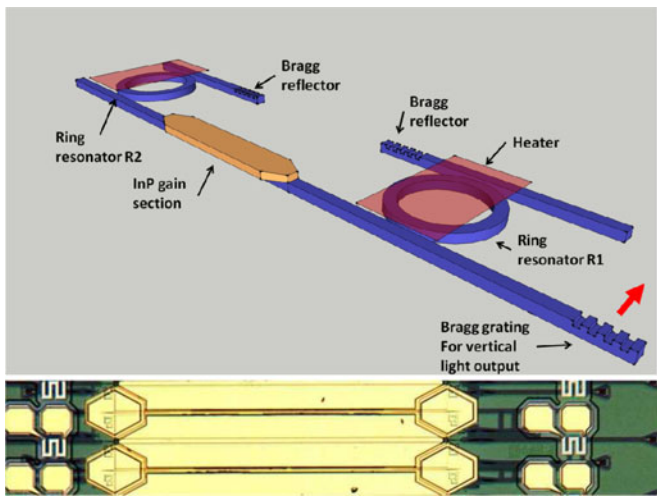


Fig. 10. Schematic view (top) and photograph (bottom) of the widely tunable single-mode hybrid laser.

reflection and output fibre coupling. The straight III–V waveguide has a width of  $1.7 \mu\text{m}$  and a length of  $500 \mu\text{m}$ . In the silicon sections, RR 1 (R1) and 2 (R2) have a free spectral range (FSR) of 650 and 590 GHz, respectively. The slight difference between these two values allows taking advantage of the Vernier effect for the wavelength tuning. Moreover, the bandwidth of the double ring filter is designed to select only one Fabry–Perot mode of the cavity. The Bragg reflectors are made by partially etching the silicon waveguide. The two Bragg reflectors, each with a pitch of 290 nm and 60 periods, are designed to have a reflectivity of more than 90%, and a 3 dB bandwidth larger than 100 nm.

In addition to the fabrication steps detailed in Section II, a NiCr metal layer is deposited on top of the RRs with contacts pads. This is to allow tuning of the RR wavelength via thermo-optic effect by heating the silicon waveguides. The last steps are the metallization for the laser contacts and heater contacts. Fig. 10 (bottom) shows a picture of the fabricated tunable lasers.

### B. Testing of Passive Circuit Elements

The passive RRs were measured on separated test samples on the same wafer area. Fig. 11 shows the transmission curves

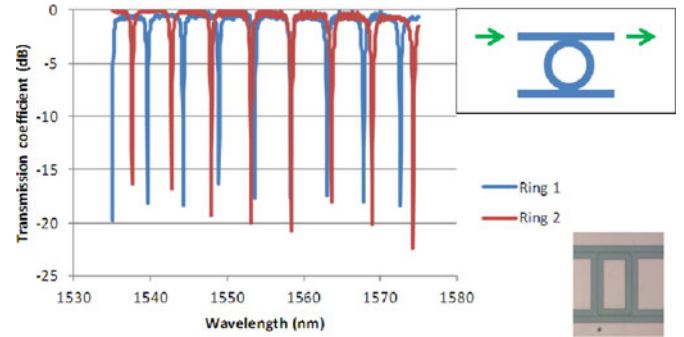


Fig. 11. Measured transmission spectra of the RRs. Inset: photo of the fabricated silicon RR.

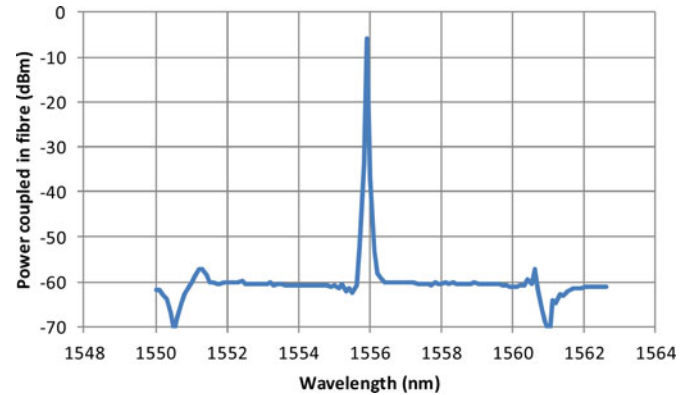


Fig. 12. Laser emission spectrum at 20 °C, 80 mA.

of the two RRs from the input port to the “through” port. Two combs of resonance peaks are observed, corresponding to the two RRs with slightly different FSRs. It is remarkable that for each resonance peak, the full width at half minimum is estimated to be around 0.5 nm. Such narrow resonance peaks show the high quality of the fabricated silicon waveguides, and are key to achieve a large tuning range with high SMSR. It is to be noted that the amplitude variation in the presented curves is due to the limited resolution bandwidth (0.07 nm) of the optical spectrum analyzer used.

### C. Laser Measurements

The lasers are tested on wafers with vertical Bragg gratings coupling the output light into a cleaved SMF. The coupling losses were measured to be around 10 dB. At 20 °C, the laser has a threshold current of 21 mA. The slope efficiency of this kind of laser is of the order of 0.1 mW/mA, leading to a differential quantum efficiency of around 8%. Fig. 12 shows the laser spectrum at 20 °C for a current of 80 mA, measured by heating the RRs. It clearly shows single-mode operation with 50 dB SMSR. Such a large SMSR is attributed to the narrow bandwidth of the RRs.

The laser linewidth was measured using a self-homodyne technique and also by a heterodyne technique through the beating with an external cavity laser. We found that the linewidth varies with the current injected into the gain region, and with the heating power applied to the RRs. Its values are in the range

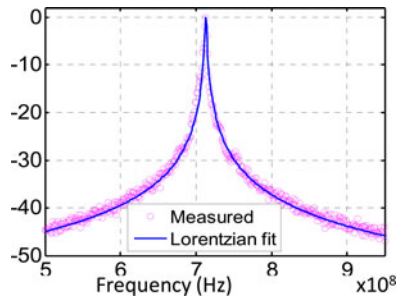


Fig. 13. Measured heterodyne spectrum through the beating with an external cavity lasers. A Lorentzian fit is also plotted.

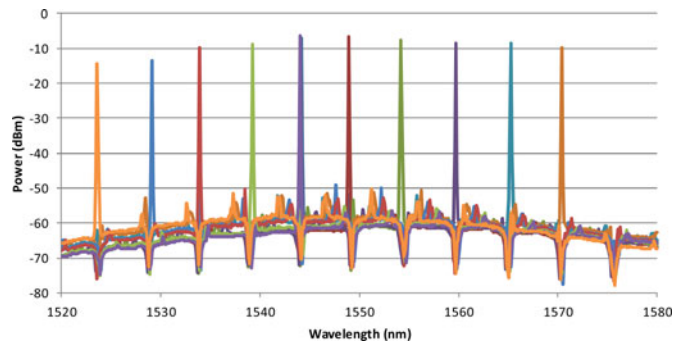


Fig. 14. Superimposed laser spectra for different currents injected into heater 1, at 20 °C, laser injection current of 80 mA. Current applied to heater 2 was fixed.

between 1 and 10 MHz. Fig. 13 shows a typical example of the measured heterodyne spectrum, with a Lorentzian fit. We can see that the lineshape is very close to a Lorentzian, and the linewidth is found to be 2.3 MHz.

Fig. 14 shows the superimposed laser emission spectra obtained by changing heating power levels applied to the two RRs. On the backgrounds of these spectra, as well as on that of Fig. 12, one can observe transmission peaks created by R2 and transmission dips created by R1. This is due to the fact that the spontaneous emission generated by the active III–V waveguide is modulated by the drop transmission of R2 and by the through transmission of R1. The power variation across the wavelength range is 6 dB and corresponds to the gain curve of the III–V material and the vertical coupler spectrum.

Fig. 15 shows the wavelength tuning curves of the laser by heating simultaneously the two RRs with a laser injection current of 80 mA at 20 °C. With less than 400 mW of combined power in both heaters, a high SMSR ( $>40$  dB) wavelength range over 45 nm is achieved. For a given power P1 in heater 1, as the power P2 in heater 2 increases, the ring peak wavelengths shifts, and the laser wavelength jumps to the next ring interference order for which the two ring resonance peaks match. For wavelength setting, both ring power must be adjusted so that one transmission peak of R1 matches the one of R2 at a desired wavelength. The wavelength tuning range is currently limited by the too large difference in the FSR between the two RRs. An optimized design should allow covering the whole gain bandwidth of the III–V active material. Also, the laser does not have a phase section and hence the wavelength is always bound to a

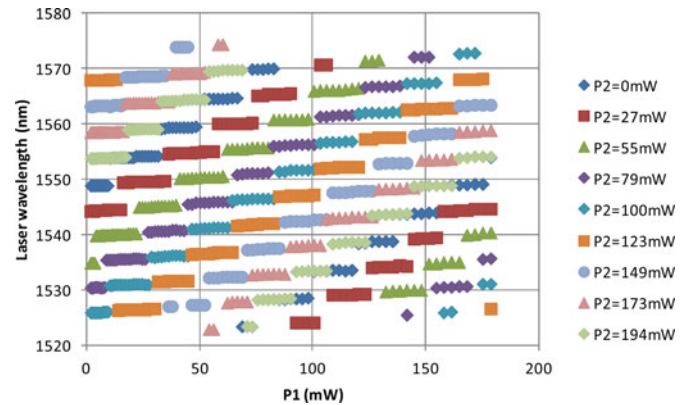


Fig. 15. Laser wavelength as a function of the electrical power in heater 1, for different electrical powers in heater 2, at 20 °C and laser injection current of 80 mA.

Fabry-Perot mode of the cavity. For a more precise wavelength tuning ( $<0.2$  nm), this laser requires adjusting of the injection current.

We demonstrated that such a hybrid III–V/Si laser can be directly modulated at 10 Gb/s [22], an interesting feature for access and metropolitan networks. Moreover, we demonstrated that such a laser can be used as a local oscillator in a coherent receiver for polarization division multiplexing-quadrature phase shift keying signal at 100 Gbit/s [22]. No penalty was observed compared to a commercially available external cavity tunable laser. Those results constitute an important milestone towards real applications of tunable hybrid III–V/Si lasers.

## V. AWG-LASER DESIGN AND FABRICATION

### A. Design

An AWG laser is a wavelength-selectable source consisting of several independent gain sections that are merged into a single output waveguide by means of an AWG inside the laser cavity, as schematically depicted in Fig. 16. Another solution to make a wavelength selectable laser source is to have an array of single frequency lasers, which are connected to an AWG outside the laser cavity. The main advantage of an AWG laser with respect to a laser array is the fact that the wavelength spacing between the different operation channels is fixed by the AWG, hence there is no need for active control of each wavelength if the device is used in a transmitter circuit.

An AWG will introduce some losses in the range between 2.5 and 6 dB in our samples. If the AWG is outside the laser cavity, the power losses are the same as the AWG losses. Now if the AWG is inside the laser cavity, the effect on laser output power can be predicted using a laser model. Our calculation showed that a 4 dB loss of an AWG will result in a decrease of the external quantum efficiency in the range between 20% and 30%. Hence the AWG laser is more efficient than the combination of a laser array and an external AWG.

First AWG lasers on an InP substrate were reported in 1996 [23], [24]. However hybrid III–V/Si integration brings new advantages for AWG lasers. As silicon based AWGs [25] have a

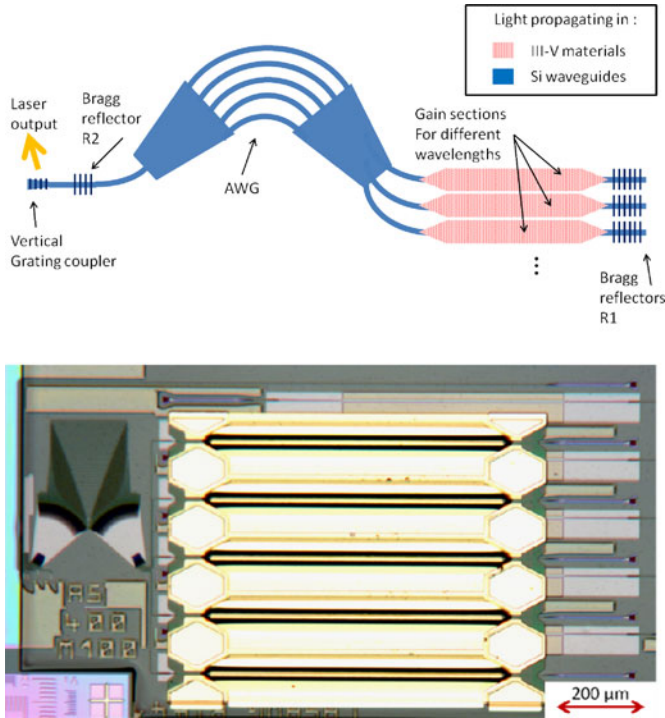


Fig. 16. (Top) Schematics and (bottom) photograph of a fabricated AWG-laser.

reduced size compared to those on InP due to the high refractive index contrast, the laser cavity becomes shorter. For instance, although deeply etched InP waveguides allowed the fabrication of very compact InP AWG lasers, the laser chip size was still  $2 \times 3 \text{ mm}^2$ , as demonstrated in [25], [26]. We report here a hybrid III-V/Si AWG laser with a footprint of  $1.4 \times 0.8 \text{ mm}^2$ . As a consequence of the smaller cavity, a high SMSR can be easier to achieve.

Fig. 16 (top) shows a schematic of the AWG laser structure. The AWG laser consists of an AWG made from SOI waveguides and III-V gain sections. The AWG has a size of  $300 \times 400 \text{ μm}^2$ . It counts 5 output channels with designed 400 GHz spacing. The designed interference order is 20, with 50 strip waveguides in the array part. To reduce the insertion losses of the filter and minimize the reflections, the tapers between the waveguides and the slab propagation region are etched in two steps [24]. The FSR is designed to be 46 nm, approximately the bandwidth of the III-V material gain curve. Such a large FSR allows a single-mode laser operation by preventing the neighboring orders from lasing. The Bragg reflectors that terminate the laser cavity are broadband; consequently they do not participate in the wavelength filtering for single-mode selection. The back reflectors R1 are longer and designed for a 99% reflectivity; the transmitted power through R1 can be used for monitoring purposes. The front reflector R2 is designed for a 30% reflectivity and closes the Fabry-Pérot cavity at the other side. At the output side, a vertical grating coupler is used to couple the output light to a cleaved single-mode fiber.

TABLE I  
LASER CHARACTERISTICS AT 20 °C FOR THE FIVE SECTIONS

Active section number	Threshold (mA)	Power coupled to single mode fibre (dBm). I=110mA	Wavelength (nm)	SMSR (dB)
			I=110mA	I=110mA
1	38	-8.6	1525.33	38
2	39	-8.9	1522.56	33
3	38	-9.5	1519.4	35
4	38	-9.9	1516.4	32
5	42	-10.9	1513.33	30

### B. Laser Measurements

The lasers are tested on wafers, using a single-mode cleaved fiber to collect the light that exits the chip through the vertical grating coupler. The test bench temperature is regulated at 20 °C. All the measurements are performed using electrical probes. The 5 SOAs of the AWG laser have a series resistance around 7 Ω. Table I shows the main characteristics of each wavelength channel biased at 110 mA. The lasing threshold remains around  $40 \pm 2$  mA for all channels, with the highest threshold corresponding to the lowest wavelength, because this channel has the largest detuning with respect to the peak gain wavelength: 1535 nm. For a given injection current (110 mA), the power coupled to the fibre ranges from -8.63 to -10.93 dBm. The coupling losses from the vertical coupler to a single-mode fiber (SMF) were measured to be in the range of 12–10 dB between 1513 and 1525 nm. Therefore, the power in the silicon output waveguide is estimated to be in the range of 1–3 mW. The corresponding differential quantum efficiency is around 5%. The high loss of the vertical coupler comes from the fact that the laser emission wavelength does not match with that of the maximum transmission. In fact, the coupler has a peak transmission around 1560 nm, and a 3 dB passband of 45 nm. The power variation with the wavelength channel can be explained by the shift between the AWG filter passband (1513 to 1525 nm) and the III-V gain peak around 1535 nm. This detuning is due to the deviation of the fabricated waveguide dimensions with respect to the designed ones. The lasing wavelengths are spaced by 392 GHz on average, with  $\pm 40$  GHz deviation. This deviation is due to the Fabry-Pérot mode selections inside the AWG passband.

Fig. 17 shows power versus injection current for each wavelength channel biased individually. The irregularities on the curve are due to mode hops. The Fabry-Pérot modes shift with injection current due to temperature effects in the SOA sections, whereas the AWG wavelengths stay constant as the test bench temperature is regulated at 20 °C. Apart from these mode hops, the AWG laser remains in a single-mode operation regime at currents up to 200 mA and temperatures up to 60 °C.

Fig. 18 shows the temperature behaviour of the laser for channel 5 between 10 °C and 60 °C. When the temperature rises, the output power coupled to the fibre remains above 0.1 mW at a bias current of 200 mA. It is remarkable that despite the thermal insulation due to the buried oxide layer and the silica bonding layer, the laser can still operate up to 60 °C in the CW regime.

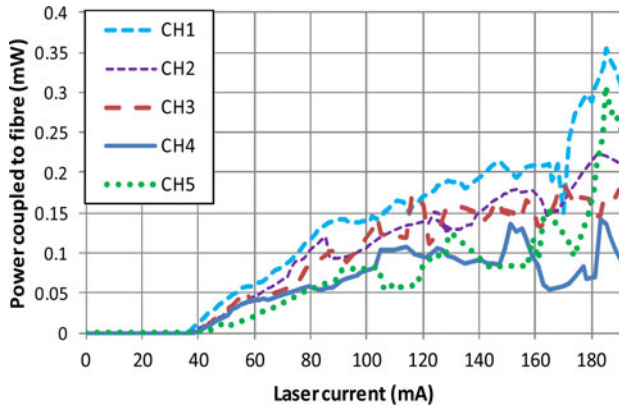


Fig. 17. Power coupled to the output fibre versus injection current for each channel at 20 °C.

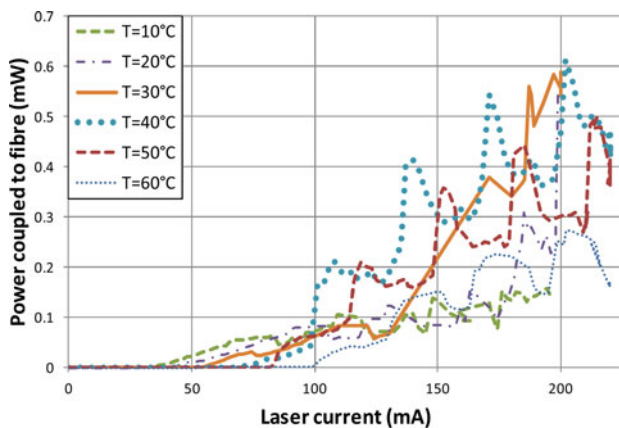


Fig. 18. Power coupled to the output fibre channel 5 versus injection current at 20 °C.

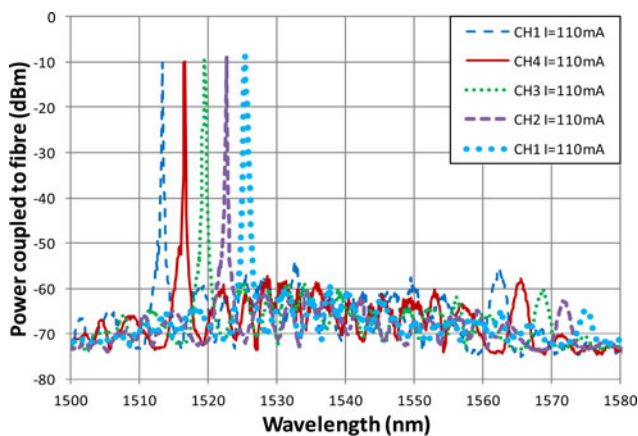


Fig. 19. Superimposed laser spectra for each channel with injection current of 110 mA at 20 °C.

Fig. 19 shows the superimposed spectra of all 5 channels when being independently biased at 110 mA. The measurements were made using an optical spectrum analyzer. As the Fabry-Pérot modes of the AWG-laser are spaced 18 GHz apart, the spectral resolution of 0.07 nm allows to verify that each channel clearly operates in a single-mode regime with an SMSR larger than 30 dB for all channels at 110 mA. Such SMSR values are

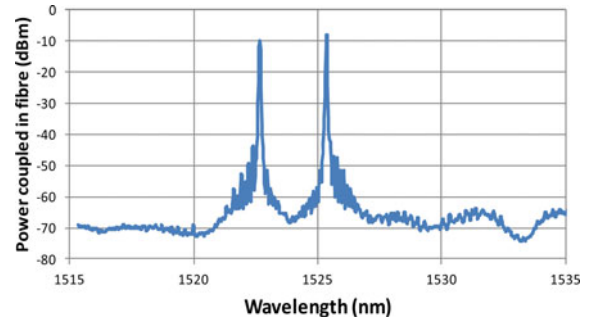


Fig. 20. Spectrum of the laser with both channel 1 and 2 being switched ON, with 110 mA current at 20 °C.

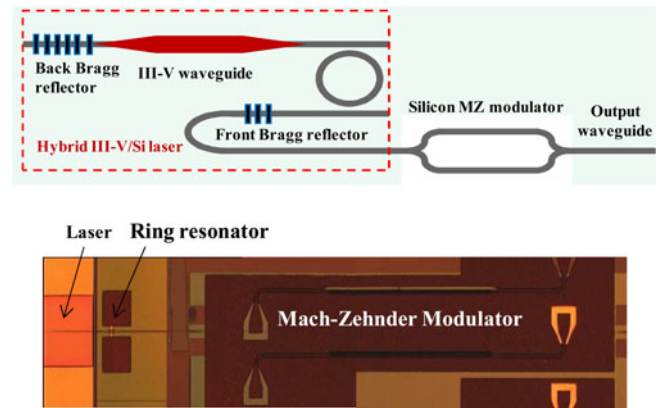


Fig. 21. Schematic view (top) and picture (bottom) of the ITLMZ chip.

already sufficient for a number of applications, although they can still be improved in future designs by decreasing the 3 dB bandwidth of the AWG filter from the current value of 190 GHz. It is also to be noted that despite the shift between the AWG filter wavelength and the maximum of the gain curve, the SMSR limited by the AWG next order in the wavelength range 1560–1575 nm remains at least 45 dB.

Fig. 20 shows the output spectrum when two channels are biased simultaneously. Both operate in a single mode regime as in the case of single channel operation. Such a behaviour shows independent operation of the two channels with negligible thermal cross-talk.

## VI. INTEGRATED TUNABLE LASER MACH-ZEHNDER MODULATOR

The developed ITLMZ chip consists of a single-mode hybrid III-V/silicon laser, a silicon MZM and an optical output coupler, as shown in Fig. 21 (top: schematic view, and bottom: a photograph). The single-mode hybrid laser includes an InP waveguide providing light amplification, and a RR allowing single-mode operation. Two Bragg reflectors etched into the silicon waveguides close the laser cavity. The MZM allows modulation of the output light emitted by the hybrid laser.

In addition to the fabrication steps outlined in Sections II (hybrid III-V/Si integration) and IV (heaters), the integration of an MZM necessitates several ion implantation steps in order to realize p++, p, n and n++ dopings.

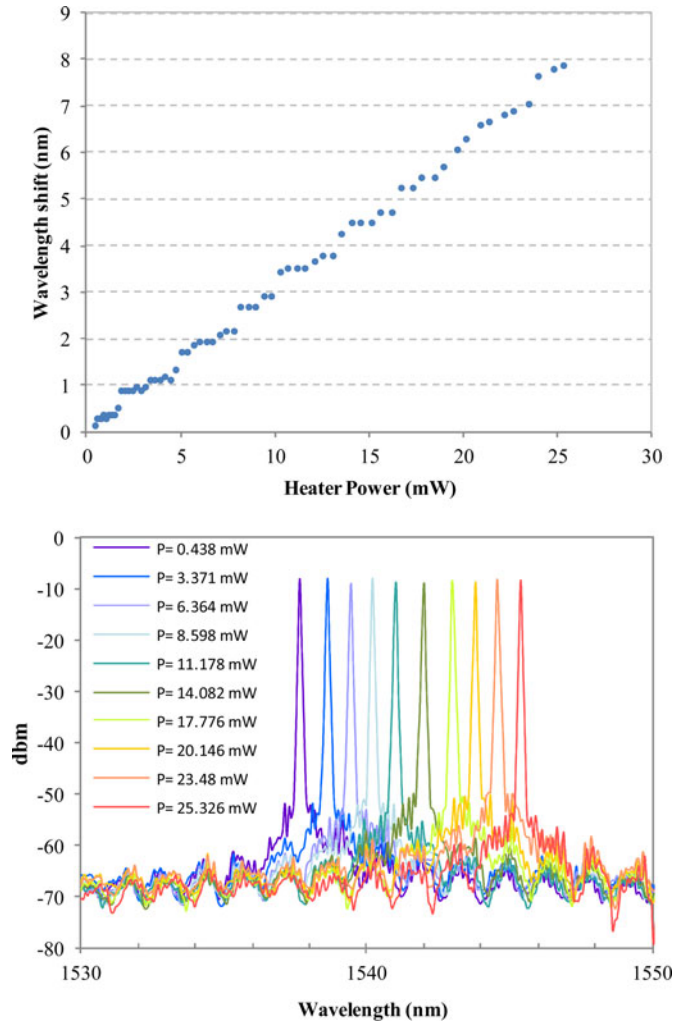


Fig. 22. Lasing wavelength as a function of the heating power (top) and super-imposed optical spectra (bottom).

#### A. Tunable Laser Characteristics

The RR-based hybrid laser exhibits a CW threshold current around 41 mA at 20 °C and the output power coupled to the silicon waveguide is around 2.5 mW for an injection current of 100 mA. The maximum output power is around 6.5 mW at 20 °C, and the output power is still higher than 1 mW at 60 °C. Electrical current injection into the heater allows thermal tuning of the ring resonance wavelength. As a result, the selected cavity mode will jump to another one having the lowest threshold [27]. Fig. 22 (top) plots the lasing wavelength as a function of the heating power. One can observe from this figure that a tuning range of 8 nm is achieved. The wavelength tuning is incremental, due to the mode jumps with the increase of heating power. This phenomenon is typical of this kind of cavity, and very similar to that observed in classical DFB Bragg lasers made on InP. The heater resistance is in the range of 20–100  $\Omega$ , and the thermal tuning efficiency is in the range of 0.15–0.4 nm/mW. Fig. 22 (bottom) shows an example of the superimposed optical spectra for 10 values of the heating power. Clearly, single-mode operation with SMSR larger than 40 dB is achieved.

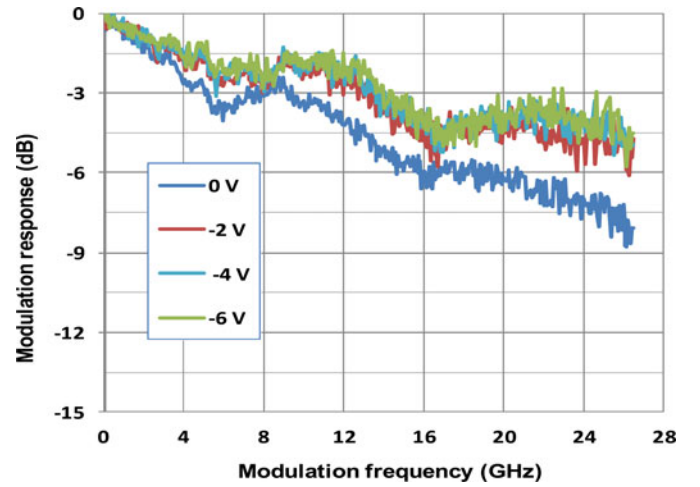


Fig. 23. Small-signal modulation response of the MZ modulator for different values of the applied voltage.

#### B. Silicon Mach-Zehnder Modulator Characteristics

The silicon modulator is a depletion type lateral pn junction modulator as described in [28]. The length of the modulated phase shifters is 3 mm. The arm length difference of the MZM is 150  $\mu\text{m}$ , resulting in a FSR of around 4.5 nm. The estimated  $V\pi L\pi$  for the modulator is around 3 V cm. The ER depends on the operation point. Its value is larger than 10 dB when the operation point is close to the minimum transmission, and 6.5 dB close to the maximum for a peak-to-peak voltage swing of 8 V. Thus the average losses are higher for the case of a larger ER. A trade-off between the losses and the ER for the modulator is made in the BER measurements. Moreover, from the power level measurement from a laser alone with the same structure and from the output of the ITLMZ chip, the intrinsic losses of the MZM are estimated to be around 13 dB at its maximum transmission point.

Fig. 23 shows the small-signal modulation response of the integrated MZM for several values of the applied voltage. One can see that the modulation bandwidth increases with the rising reverse bias voltage of the pn junction due to a reduction of the capacitance with voltage. For a reverse bias larger than 2 V, the 3 dB modulation bandwidth is larger than 13 GHz. The modulation response decreases very slowly with the modulation frequency. Such a modulation response guarantees operation at 10 Gb/s, and should allow modulation at bit rates up to 25 Gb/s.

#### C. BER Measurement of the ITLMZ

The output of the ITLMZ chip is coupled to a lensed fiber, amplified by an erbium doped fiber amplifier and then filtered out. One arm of the MZM is modulated with a voltage swing of around 7 V, at 10 Gb/s using a pseudo-random binary sequence (PRBS). The BER measurement is performed for 8 different wavelengths distributed inside the tuning range by changing the power dissipated in the RR heater [18]. Fig. 24 shows the BER curves for all the wavelengths and also a reference curve for a directly modulated laser, measured using a high sensitivity receiver including an avalanche photodiode. The PRBS length

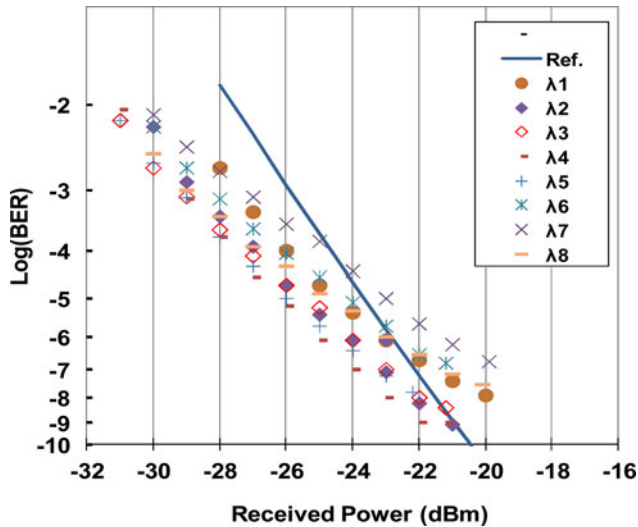


Fig. 24. Bit error rate for different wavelengths.

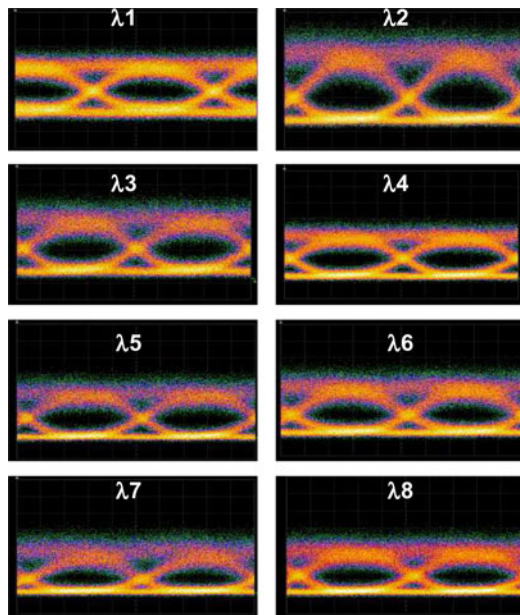


Fig. 25. Eye diagrams for different wavelengths.

is  $2^7-1$ , limited by the photo-receiver used in this experiment. Fig. 25 shows the corresponding eye diagram for all those channels, independent of the length of PRBS in the range from  $2^7-1$  to  $2^{31}-1$ . The ER of the different wavelengths varies from 6 to 10 dB, while the ER for the reference is only 4 dB. One can see from Fig. 4 that all channels have better BER performance than the reference for received power levels lower than  $-25$  dBm, due to the higher ER of the ITLMZ compared to that of the reference. For power levels higher than  $-25$  dBm, channels  $\lambda_2$ ,  $\lambda_3$ ,  $\lambda_4$  and  $\lambda_5$  behave slightly better than the reference, achieving error-free operation with  $\text{BER} < 10^{-9}$ . Other channels have minimum BER between  $10^{-7}$  and  $10^{-8}$ , mainly limited by the optical signal to noise ratio (OSNR) due to the high coupling losses between the ITLMZ output waveguide and the lensed fiber used. The power level difference to achieve the same BER

among all channels is around 4 dB, explained by the difference in OSNR and the achieved ER among those channels. Finally, the smaller slopes for all wavelength channels compared to that of the reference in the BER curves is attributed to their lower OSNR

## VII. CONCLUSION

Heterogeneous integration of III-V on silicon seems to be a very promising way to fabricate laser sources on silicon. Large progress has been made on the performance of the fabricated III-V on silicon lasers. Moreover, the silicon waveguides enable additional functionalities such as spectral filtering in a DBR laser or wavelength-tuning in lasers with integrated RRs. The integration of hybrid lasers on silicon further allows the fabrication of more complete photonic circuits such as transmitters and receivers.

However, some improvements on laser performance are still to be made in order to reach specifications for practical applications. For instance, the slope efficiency of the hybrid lasers reported in this paper is in the range of  $0.1 - 0.15$  mW/mA range for  $400 \mu\text{m}$  length devices. There is still a factor between 2 and 3 to be improved in order to compete with the state of the art monolithically integrated InGaAsP lasers on InP substrate. In terms of thermal behavior, measurements on our lasers showed that thermal impedance is in the range of  $120$  K/W for devices with a length of  $400 \mu\text{m}$ . With an injection current of  $100$  mA, the temperature increase is around  $20$  K. There are basically two ways to improve the thermal performance. The first one is the thermal management. For instance, a thermal “shunt” was introduced into a device by etching away the  $\text{SiO}_2$  and silicon epitaxial layers, and backfilling the etched regions with high thermal conductivity material [29]. It is also possible to introduce some heat sinks on the top of III-V lasers, for example, very thick metallic layers for the electrodes. The second approach is to use much less temperature sensitive III-V materials such as quantum dots as the gain material inside the laser cavity.

Another important development direction of hybrid III-V lasers on silicon is the demonstration of DFB type single frequency lasers. Such lasers present the advantage of maintaining the single frequency behavior without mode hopping due to temperature or injection current variations. They can have a number of applications in particular for short range optical communications, in which active temperature control is to be avoided. Most lasers (DBR lasers, tunable lasers and AWG lasers) presented in this paper have mode jumps when the temperature or injection current varies. Those lasers are more suitable for applications in which active temperature control can be applied.

## REFERENCES

- [1] C. Gunn, “CMOS photonics for high-speed interconnects,” *IEEE Micro*, vol. 26, no. 2, pp. 58–66, Mar./Apr. 2006.
- [2] R. Soref, “The Past, Present, and Future of Silicon Photonics,” *IEEE J. Sel. Topics Quantum Electron.*, vol. 12, no. 6, pp. 1678–1687, 2006.
- [3] P. Dong, Y.-K. Chen, G.-H. Duan, and D. T. Neilson, “Silicon photonic devices and integrated circuits,” *J. Nanophotonics*, to be published.
- [4] J. F. Liu, X. Sun, R. Camacho-Aguilera, L. C. Kimerling, and J. Michel, “A Ge-on-Si laser operating at room temperature,” *Opt. Lett.*, vol. 35, pp. 679–681, Mar. 2010.

- [5] R. E. Camacho-Aguilera, Y. Cai, N. Patel, J. T. Bessette, M. Romagnoli, L. C. Kimerling, and J. Michel, "An electrically pumped germanium laser," *Opt. Exp.*, vol. 20, no. 10, pp. 11316–11320, 2012.
- [6] A. W. Fang, H. Park, Y.-H. Kuo, R. Jones, O. Cohen, D. Liang, O. Rada, M. N. Sysak, M. J. Paniccia, and J. E. Bowers, "Hybrid silicon evanescent devices," *Mater. Today*, vol. 10, no. 7–8, pp. 28–35, 2007.
- [7] G. Roelkens, J. Van Campenhout, J. Brouckaert, D. Van Thourhout, R. Baets, P. Rojo Romeo, P. Regreny, A. Kazmierczak, C. Seassal, X. Letartre, G. Hollinger, J.-M. Fedeli, L. Di Cioccio, and C. Lagahe-Blanchard, "III-V/Si photonics by die-to-wafer bonding," *Mater. Today*, vol. 10, no. 7–8, pp. 36–43, 2007.
- [8] H. Park, M. N. Sysak, H.-W. Chen, A. W. Fang, D. Liang, L. Liao, B. R. Koch, J. Bovington, Y. Tang, K. Wong, M. Jacob-Mitos, R. Jones, and J. E. Bowers, "Device and integration technology for silicon photonic transmitters," *IEEE J. Sel. Topics Quantum Electron.*, vol. 17, no. 3, pp. 671–688, May/Jun. 2011.
- [9] B. Ben Bakir, A. Descos, N. Olivier, D. Bordel, P. Grosse, E. Augendre, L. Fulbert, and J.-M. Fedeli, "Electrically driven hybrid Si/III-V lasers based on adiabatic mode transformers," *Opt. Exp.*, vol. 19, no. 11, pp. 10317–10325, 2011.
- [10] M. Lamponi, S. Keyvaninia, C. Jany, F. Poingt, F. Lelarge, G. de Valicourt, G. Roelkens, D. Van Thourhout, S. Messaoudene, J.-M. Fedeli, and G. H. Duan, "Low-threshold heterogeneously integrated InP/SOI laser with a double adiabatic taper coupler," *IEEE Photon. Technol. Lett.*, vol. 24, no. 1, pp. 76–78, Jan. 2012.
- [11] A. Le Liepvre, C. Jany, A. Accard, M. Lamponi, F. Poingt, D. Make, F. Lelarge, J.-M. Fedeli, S. Messaoudene, D. Bordel, and G.-H. Duan, "Widely wavelength tunable hybrid III-V/silicon laser with 45 nm tuning range fabricated using a wafer bonding technique," in *Proc. IEEE 9th Int. Conf. Group IV Photon.*, Aug. 29–31, 2012, pp. 54–56.
- [12] B. R. Koch, E. J. Norberg, B. Kim, J. Hutchinson, J.-H. Shin, G. Fish, and A. Fang, "Integrated silicon photonic laser sources for telecom and datacom," presented at the Opt. Fiber Commun. Conf., Anaheim, CA, USA, Mar. 2013.
- [13] E. Marchena, T. Creazzo, S. B. Krasulick, P. K. L. Yu, D. Van Orden, J. Y. Spann, C. C. Blivin, J. M. Dallesasse, P. Varangis, R. J. Stone, and A. Mizrahi, "Integrated tunable CMOS laser for Si photonics," presented at the Opt. Fiber Commun. Conf., Anaheim, CA, USA, Mar. 2013.
- [14] G. Kurczveil, M. J. Heck, J. D. Peters, J. M. Garcia, D. Spencer, and J. E. Bowers, "An integrated hybrid silicon multiwavelength AWG laser," *IEEE J. Sel. Topics Quantum Electron.*, vol. 17, no. 6, pp. 1521–1527, Nov./Dec. 2011.
- [15] A. Le Liepvre, A. Accard, F. Poingt, C. Jany, M. Lamponi, D. Make, F. Lelarge, J.-M. Fedeli, S. Messaoudene, D. Bordel, and G.-H. Duan, "A wavelength selectable hybrid III-V/Si laser fabricated by wafer bonding," *IEEE Photon. Technol. Lett.*, vol. 25, no. 16, pp. 1582–1585, Aug. 2013.
- [16] S. Keyvaninia, S. Verstuyft, S. Pathak, F. Lelarge, G. H. Duan, D. Bordel, J. M. Fedeli, T. De Vries, B. Smalbrugge, E. J. Geluk, J. Bolk, M. Smit, G. Roelkens, and D. Van Thourhout, "III-V-on-silicon multi-frequency lasers," *Opt. Exp.*, vol. 21, no. 11, pp. 13675–13683, 2013.
- [17] A. Alduino, L. Liao, R. Jones, M. Morse, B. Kim, W.-Z. Lo, J. Basak, B. Koch, H.-F. Liu, H. Rong, M. Sysak, C. Krause, R. Saba, D. Lazar, L. Horwitz, R. Bar, S. Litski, A. Liu, K. Sullivan, O. Dosunmu, N. Na, T. Yin, F. Haubensack, I.-W. Hsieh, J. Heck, R. Beatty, H. Park, J. Bovington, S. Lee, H. Nguyen, H. Au, K. Nguyen, P. Merani, M. Hakami, and M. Paniccia, "Demonstration of a high speed 4-channel integrated silicon photonics WDM link with hybrid silicon lasers," presented at the Integr. Photon. Res., Silicon Nanophoton., Monterey, CA, USA, 2010.
- [18] G.-H. Duan, C. Jany, A. Le Liepvre, J.-G. Provost, D. Make, F. Lelarge, M. Lamponi, F. Poingt, J.-M. Fedeli, S. Messaoudene, D. Bordel, S. Brisson, S. Keyvaninia, G. Roelkens, D. Van Thourhout, D. J. Thomson, F. Y. Gardes, and G. T. Reed, "10 Gb/s integrated tunable hybrid III-V/Si laser and silicon Mach-Zehnder modulator," presented at the Eur. Conf. Opt. Commun., Amsterdam, The Netherlands, Sep. 2012.
- [19] J.-M. Fedeli, B. Ben Bakir, N. Olivier, P. Grosse, L. Grenouillet, E. Augendre, P. Philippe, K. Gilbert, D. Bordel, and J. Harduin, "InP on SOI devices for optical communication and optical network on chip," *Proc. SPIE Photon. West Conf., Optoelectron. Integr. Circuits XIII*, vol. 7942, pp. 794200-1–794200-9, 2011.
- [20] D. Bordel, M. Argoud, E. Augendre, J. Harduin, P. Philippe, N. Olivier, S. Messaoudene, K. Gilbert, P. Grosse, B. Ben Bakir, and J.-M. Fedeli, "Direct and polymer bonding of III-V to processed silicon-on-insulator for hybrid silicon evanescent lasers fabrication," *ECS Trans.*, vol. 33, pp. 403–410, 2010.
- [21] A. J. Zilkie, P. Seddighian, B. J. Bijlani, W. Qian, D. C. Lee, S. Fatholouloumi, J. Fong, R. Shafiiha, D. Feng, B. J. Luff, X. Zheng, J. E. Cunningham, A. V. Krishnamoorthy, and M. Asghari, "Power-efficient III-V/silicon external cavity DBR lasers," *Opt. Exp.*, vol. 20, pp. 23456–23462, 2012.
- [22] G. de Valicourt, A. Leliepre, F. Vacondio, C. Simonneau, C. Jany, A. Accard, F. Lelarge, M. Lamponi, D. Make, F. Poingt, G. H. Duan, J.-M. Fedeli, S. Messaoudene, D. Bordel, L. Lorcy, J.-C. Antona, and S. Bigo, "Directly modulated and fully tunable hybrid silicon lasers for future generation of coherent colorless ONU," *Opt. Exp.*, vol. 20, pp. B552–B557, 2012.
- [23] M. Zirngibl, C. H. Joyner, C. R. Doerr, L. W. Stultz, and H. M. Presby, "An 18-channel multifrequency laser," *IEEE Photon. Technol. Lett.*, vol. 8, no. 7, pp. 870–872, Jul. 1996.
- [24] A. Staring, L. Spiekman, J. J. M. Binsma, E. J. Jansen, T. Van Dongen, P. J. A. Thijs, M. K. Smit, and B. H. Verbeek, "A compact nine-channel multiwavelength laser," *IEEE Photon. Technol. Lett.*, vol. 8, no. 9, pp. 1139–1141, Sep. 1996.
- [25] W. Bogaerts, P. Dumon, D. V. Thourhout, D. Taillaert, P. Jaenen, J. Wouters, S. Beckx, V. Wiaux, and R. G. Baets, "Compact wavelength-selective functions in silicon-on-insulator photonic wires," *IEEE J. Select. Topics Quantum Electron.*, vol. 12, no. 6, pp. 1394–1401, Nov.-Dec. 2006.
- [26] M. J. R. Heck, A. La Porta, X. J. M. Leijts, L. M. Augustin, T. De Vries, B. Smalbrugge, O. Yok-Siang, R. Notzel, R. Gaudino, D. J. Robbins, and M. K. Smit, "Monolithic AWG-based discretely tunable laser diode with nanosecond switching speed," *IEEE Photon. Technol. Lett.*, vol. 21, no. 13, pp. 905–907, Jul. 1, 2009.
- [27] S. Keyvaninia, G. Roelkens, D. Van Thourhout, C. Jany, M. Lamponi, A. Le Liepvre, F. Lelarge, D. Make, G. Duan, D. Bordel, and J. Fedeli, "Demonstration of a heterogeneously integrated III-V/SOI single wavelength tunable laser," *Opt. Exp.*, vol. 21, pp. 3784–3792, 2013.
- [28] D. J. Thomson, F. Y. Gardes, Y. Hu, G. Mashanovich, M. Fournier, P. Grosse, J.-M. Fedeli, and G. T. Reed, "High contrast 40Gbit/s optical modulation in silicon," *Opt. Exp.*, vol. 19, pp. 11507–11516, 2011.
- [29] M. N. Sysak, D. Liang, R. Jones, G. Kurczveil, M. Piels, M. Fiorentino, R. G. Beausoleil, and John E. Bowers, "Hybrid silicon laser technology: A thermal perspective," *IEEE J. Sel. Topics Quantum Electron.*, vol. 17, no. 6, pp. 1490–1498, 2011.



**Guang-Hua Duan** (S'88–M'90–SM'01) received the B.E. degree from Xidian University, Xi'an, China, in 1983, the M.E. and Doctorate degrees from the Ecole Nationale Supérieure des Télécommunications (Telecom-ParisTech), Paris, France, in 1987 and 1991, respectively, all in applied physics. He was habilitated to direct researches by Université de Paris-Sud in 1995. He is now the Leader of the research team "Silicon Photonics" within III-V Lab, which is a joint laboratory of "Alcatel-Lucent Bell Labs France," "Thales Research and Technology,"

and "CEA Leti." He is author or coauthor of more than 100 journal papers, 200 conference papers, 25 patents, and a contributor to three book chapters. He is also a Guest Professor in Ecole Supérieure d'Electricité, Paris, France, and Ecole Supérieure d'Optique, Palaiseau, France, giving lectures in the fields of electromagnetism, optoelectronics, and laser physics.

**Christophe Jany** received the Ph.D. degree in materials science from the University of Paris XII, Créteil, France, in 1998. He studied thin film technology of CVD Diamond on Silicon. He joined Alcatel Research & Innovation Center in Marcoussis in 1999. He has been engaged in the development of optical integration technology of III-V semiconductors components, including high speed (> 40 Gb/s) integrated lasers and electro-absorption modulators. Within Bell Labs France, he contributed to the development of new InP-based platforms integration using SAG and SIBH Technologies. So, he is currently with the III-V Lab, leading expert in the field of photonic integration with more than 13 years of experience in the field of InP-based Photonic Integrated Circuits. For three years, he developed the hybrid technology III-V on SOI, leading to the Silicon Photonics chips (Laser source). His main focus is to make compatible manufacturing III-V materials on "CMOS" material.

**Alban Le Liepvre**, photograph and biography not available at the time of publication.

**Alain Accard**, photograph and biography not available at the time of publication.



**Marco Lamponi** was born in Terni, Italy, in 1984. He received the M.Sc. degree in physical engineering from the Politecnico di Milano, Milan, Italy, and the French diploma of electrical engineering from the Ecole Supérieure d'Electricité, Paris, France, in 2008, and the M.Sc. degree in nano-science and micro-systems and the Ph.D. degree from Paris-sud University, Orsay, France, in 2012. His doctoral work focused on the design and fabrication of hybrid III-V on silicon lasers. He got a permanent position in January 2012 at the III-V Lab, Palaiseau, France, to

work on III-V photonic integrated circuits and high power lasers.

**Dalila Make**, photograph and biography not available at the time of publication.



**Peter Kaspar** received the M.Sc. and Ph.D. degree in physics from ETH Zurich, Zurich, Switzerland, in 2005 and 2012, respectively. In 2005, he was with the Ultrafast Laser Physics Laboratory, ETH Zurich, where he worked on high harmonic generation in noble gases using ultrashort laser pulses. From 2006 to 2012, he was with the Communication Photonics Group, Electronics Laboratory, ETH Zurich, where he studied nanostructured photonic elements and developed III-V semiconductor technology for active photonic crystal devices. He joined III-V Lab, Palaiseau, France, in 2013, to work on hybrid lasers and SOAs (III-V on silicon) for photonic integrated circuits on silicon.

**Guillaume Levaufre** received the Master's degree of engineering in optoelectronics from INSA Rennes, Rennes, France, in 2012. The same year, he made an internship at the III-V Lab, working on inductively coupled plasma etching of InP. Since October 2012, he has been working toward the Ph.D. degree with Alcatel-Lucent Bell Labs at the III-V Lab. His research work is focused on hybrid III-V/Silicon photonic integrated circuits for high-speed telecommunications.

**Nils Girard** received the Master's degree of engineering (option: photonics) from SUPELEC, Gif-Sur-Yvette, France, and the Master of Science degree (Physics, Plasma, Photonics) from the University of Metz-Nancy, Metz, France, in 2012. Later this year, he was with Thales Research and Technology on the generation of RF signal with dual-frequency VECSEL. He started the Ph.D. research with the III-V Lab, Palaiseau, France, in November 2012 to work on low noise hybrid III-V/silicon lasers for radar and ultrastable clocks applications.



**François Lelarge** received the Diploma in material science and the Ph.D. degree, both from the University of Pierre et Marie Curie, Paris, France, in 1993 and 1996, respectively. From 1993 to 1996, he was with the Laboratory of Microstructures and Microelectronic, CNRS Bagneux, Paris, France. His thesis work was devoted to the fabrication and the optical characterization of GaAs/AlAs lateral superlattice grown on vicinal surfaces by MBE. From 1997 to 2000, he was a Postdoctoral Researcher at the Institute of Micro and Optoelectronics, Lausanne, Switzerland. He worked on InGaAs/GaAs quantum wires fabrication by MOCVD regrowth on patterned substrates. He is currently the Incharge of the Epitaxy and New Material Technology team within the III-V Lab and coordinator of a project on QD-based directly modulated lasers (ANR-DIQDOT).



**Jean-Marc Fedeli** received his electronics engineer diploma from INPG Grenoble in 1978. Then he conducted researches at the CEA-LETI on various magnetic memories and magnetic components as project leader, group leader, and program manager. For two years, he acted as advanced program director in Memscap company for the development of RF-MEMS, then he returned to CEA-LETI in 2002 as coordinator of silicon photonic projects up to 2012. Under a large partnership with universities and research laboratories, he works on various technological aspects on Photonics on CMOS (Si rib and stripe waveguides, Si<sub>3</sub>N<sub>4</sub> and a-Si waveguides, slot waveguides), Si modulators, Ge photodetectors, InP sources on Si. His main focus was on the integration of a photonic layer at the metallization level of an electronic circuit. He has been participating on different European FP6 projects (PICMOS, PHOLOGIC, MNTE, ePIXnet). Under the European FP7, he was involved in the WADIMOS, PhotonFAB (ePIXfab) projects and was program manager of the HELIOS project. He is currently managing the FP7 PLAT4M project on Silicon Photonics Platform and involved in industrial projects on Silicon Photonics.

**Antoine Descos**, photograph and biography not available at the time of publication.

**Badhise Ben Bakir**, photograph and biography not available at the time of publication.

**Sonia Messaoudene**, photograph and biography not available at the time of publication.

**Damien Bordel**, photograph and biography not available at the time of publication.



**Sylvie Menezo** graduated from INSA Lyon (France) in material sciences. In 1999, she received the Ph.D. degree in optoelectronics, from the Centre National d'Etude des Télécommunications (France Telecom), and then joined Alcatel Corporate Research Center (France), where she completed a transfer of a laser pump to Alcatel Optronics production lines. Besides telecom applications, she has worked on seismic fiber optic sensing applications with the company Sercel (Compagnie Générale de Géophysique) for 8 years where she led the Optical technologies R&D lab (France & USA). She joined CEA-Leti (France) in 2010, having, as main topics of research, design and prototyping of optical communication links based on Silicon Photonics devices. She is currently leading the Silicon photonics lab at CEA-Leti, and the IRT Nanoelec-Photonics French project.

**Guilhem de Valicourt** received the B.Sc. degree in applied physics from the National Institute of applied Sciences, Toulouse, France, in 2008. From 2007 to 2008, he followed and passed the Master's of Science degree in photonics devices from Essex University, Colchester, U.K. In 2008, he joined III-V lab, where he was working on design, fabrication, and characterization of Reflective SOA and directly modulated DFB lasers for microwave photonic systems and next generation of optical access networks toward the Ph.D. degree. In 2011, he joined Alcatel-Lucent Bell Labs in France as a Research Engineer. His main research interests are focused on the study of advanced integrated photonics devices (in InP, silicon and hybrid III-V on silicon platform) for optical packet transport and switching for metropolitan and wireless backhaul networks as well as for datacenters and access networks. He has authored or coauthored more than 50 scientific papers in journals and international conferences, two book chapters, and holds 15 patents. Dr. Valicourt received the 2011 "Best project" award from Alcatel-Lucent Bootcamp, the Marconi Young Scholar 2012 award, and was finalist for the ParisTech Ph.D. prize 2012.



**Shahram Keyvaninia** received the degree in applied physics and the M.Sc. degree in Photonics from Sharif University of Technology and ICST, Tehran, Iran. He has been working toward the Ph.D. degree from Photonic Research Group, Interuniversity Microelectronics Center/Ghent University, Ghent, Belgium, since 2008. He developed the technology for integrating III-V material on top of silicon-on-insulator (SOI) based on die-to-wafer bonding and new fabrication processes for photonic devices. His current research interests include the design, fabrication, and characterization of integrated photonic devices and heterogeneous integration of InP-on-silicon. Mr. Keyvaninia is a student member of IEEE Laser and Electrooptics Society and Optical Society of America.

**Gunther Roelkens** graduated as an electronics engineer (option: microelectronics and opto-electronics) (Hons.) from Ghent University, Ghent, Belgium, in 2002. Since 2002, he has been working in the Photonics Research Group at Ghent University, where he received the doctoral degree in April 2007, for his work in the field of heterogeneous III-V/silicon photonics. In this work, the technology for integrating III-V material on top of silicon-on-insulator waveguide circuits was developed and the integration of thin film III-V laser diodes and photodetectors on top of and coupled to the SOI waveguide circuit was demonstrated. He is currently a Tenure Track Professor in the same group. His research interests include heterogeneous III-V/silicon integration, efficient fiber-chip coupling, all-optical signal processing, and mid-infrared photonic integrated circuits.

**Dries Van Thourhout**, photograph and biography not available at the time of publication.

**David J. Thomson** started his silicon photonics research as a Ph.D. degree student at the University of Surrey, Surrey, U.K., under the guidance of Prof. Graham Reed, in 2004. His Ph.D. degree project involved investigating silicon based total internal reflection optical switches and more specifically methods of restricting free carrier diffusion within such devices. He is currently is a Senior Research Fellow in the Optoelectronics Research Centre at the University of Southampton, Southampton, U.K. His research interests include optical modulation, optical switching, integration, and packaging in silicon. In 2008, he took up a role as a Research Fellow in the same research group leading the work package on silicon optical modulators within the largest European silicon photonics project named HELIOS. Within this project, he designed the first silicon optical modulator operating at 50Gbit/s. In 2011, he presented invited talks at SPIE Photonics West and IEEE Group IV Photonics conferences and in 2012 was selected to present his work at the SET for Britain event in the Houses of Parliament.

**Frederic Y. Gardes** received the B.Sc. degree from the University of Portsmouth in 2001, the Master degree from Northumbria University in 2002, and the Ph.D. degree from the University of Surrey in 2008. He is currently an Academic Fellow appointed as a Lecturer in the School of Electronics and Computer Science, University of Southampton, Southampton, U.K. He is conducting his research as part of the Optoelectronics Research Centre. His previous research covers silicon photonics and particularly high speed active optical devices in silicon and germanium. In 2005, He initiated work on silicon optical depletion modulators and was the first to predict operation above 40 GHz. In 2011, he and his collaborators demonstrated optical modulation of up to 50 Gb/s and a 40 Gb/s modulator with a quadrature extinction ratio (ER) of 10dB setting a new state of the art performance in both speed of modulation in silicon devices and ER. He is currently working with several national and international collaborators in two large research programs where he leads the research effort in optical modulators and detector integration. These programmes are the £5M U.K. Silicon Photonics project funded by EPSRC, and the £8M EU FP7 HELIOS. He is also involved in photonic crystal slow light, ultralow power nano-cavity modulators, silicon/germanium QCSE devices, germanium and defect induced detectors in silicon and active device integration in group IV materials. He has authored more than 80 publications and five book chapters in the field of Silicon Photonics. He has also been involved in the FP6 ePIXnet program and is a regular invited and contributing author to the major Silicon Photonics conferences around the world. He is also a member of the programme committee of the IEEE Group IV Photonics conference.

**Graham T. Reed** received the Ph.D. degree in 1987. He is currently a Professor of Silicon Photonics and Group Leader. He has recently joined Southampton from the University of Surrey, where he was a Professor of Optoelectronics, and was the Head of the Department of Electronic Engineering from 2006 to 2012. He is a pioneer in the field of silicon photonics, and acknowledged as the individual who initiated the research field in the U.K. He established the Silicon Photonics Research Group at Surrey in 1989. The first Silicon Photonics company in the world, Bookham Technology Inc., was founded by Reed's Ph.D. student, Dr. Andrew Rickman, and adopted the research developed in the Group. The Silicon Photonics Group have provided a series of world leading results since its inception, and are particularly well known for their work on silicon optical modulators. For example, the group produced the first published design of an optical modulator with a bandwidth exceeding 1 GHz, and were the first to publish the design of a depletion mode optical modulator, which is now a technology standard device. More recently the team were responsible for the first all-silicon optical modulator operating at 40 Gb/s with a high extinction ratio (10dB), as well as a second modulator design (also operating at 40 Gb/s) that operates close to polarization independence. They have now reported the first device operating at 50 Gb/s. He is a regular invited and contributing author to the major Silicon Photonics conferences around the world. He has served on numerous international conference committees, and has also chaired many others. To name but two, he has been the Cochair of the Silicon Photonics symposium at Photonics West since it was first established in 2006, and in 2011, he was the Cochair of the prestigious Silicon Photonics conference, IEEE Group IV Photonics, held at the Royal Society in London. He is currently a member of five international conference committees, and has published more than 250 papers in the field of Silicon Photonics. He will Cochair four international symposia/conferences in 2012.